Cesalea N. Osborne, David J. Keeling, Jason S. Polk, Patricia N. Kambesis, and Kevin B. Cary. Land-use impacts on the hydrology of the Hidden River groundwater subbasin, Horse Cave, Hart County, Kentucky. *Journal of Cave and Karst Studies*, v. 84, no. 1, p. 27-40. DOI:10.4311/2021ES0107

LAND-USE IMPACTS ON THE HYDROLOGY OF THE HIDDEN RIVER GROUNDWATER SUBBASIN, HORSE CAVE, HART COUNTY, KENTUCKY

Cesalea N. Osborne[1,2*], David J. Keeling[1], Jason S. Polk[1], Patricia N. Kambesis[1], and Kevin B. Cary[1]

Abstract

Hidden River Cave, located in the city of Horse Cave, Ky., forms one of the main tributaries of the Hidden River groundwater subbasin that spans multiple counties in south-central Kentucky. Hidden River Cave formed in Mississippian-aged carbonates and consists of a dendritic network of canyons and collapsed domes; a major trunk stream flows through the cave that supports myriad subsurface ecosystems and recharges the Mammoth Cave aquifer and the Green River, important water resources on which several communities depend. Poor land-use practices historically have contaminated the cave stream. As a result, the hydrology of the Hidden River groundwater subbasin has been extensively studied using fluorescent dye-tracing, and developments in groundwater resource management have improved cave conditions. However, land-use boundaries that intersect with areas of recharge still influence contaminant transport to groundwater. This study combined groundwater dye-tracing, high-resolution stage data collection, and supervised classification in a geographic information system (GIS) to assess land-use impacts on the hydrology of the Hidden River groundwater subbasin. Dye-tracing confirmed that stormwater infrastructure in Horse Cave discharges to Hidden River Cave, and, subsequently, the Hidden River groundwater subbasin. High-resolution stage data determined that the cave's major trunk streams respond to precipitation within 40 minutes to 1.5 hours, while baselevel conditions, except after sustained precipitation, are met three to four days after precipitation ends. Supervised classification determined that development is concentrated in Horse Cave and has increased by approximately 7 % between 1989 and 2017. These results suggest opportunities for the implementation of karst-specific stormwater management regulations where such regulations are weak.

INTRODUCTION

Institutional policies that govern groundwater management at local, regional, and global scales often are either lacking or absent, which is particularly true, and even more challenging, where aquifers span the geographic boundary of multiple political territories. Approximately 263 transboundary groundwater resources exist globally, many of which lie in karst regions (Jarvis et al., 2005). Karst, characterized by the chemical dissolution of carbonate bedrock, comprises 15−20 % of the Earth's ice-free landscape and includes karst aquifers, which provide 25 % of the world's population with drinking water (Ford and Williams, 2007; Palmer, 2007). In karst regions, surface and groundwater flow are highly interconnected, and drainage occurs rapidly through conduits created by dissolution. Thus, the distribution and availability of groundwater resources is highly variable. Further, contaminants that enter the subsurface of karst regions can easily be dispersed throughout the groundwater system and across political boundaries.

Some of the challenges associated with policy development regarding transboundary karst aquifers include a limited understanding of recharge and discharge mechanics and uncertainties in the spatial and temporal components of subsurface flow (Theesfeld, 2010; Milanović, 2016). Some transboundary karst aquifers (i.e., the Dinaric, Yucatán Peninsula, and Arbuckle-Simpson karst aquifers) have benefited from hydrogeologic studies, such as groundwater dye-tracing and the development of groundwater flow models, to characterize subsurface flow (Bauer-Gottwein et al., 2011; Christenson et al., 2011; Stevanović et al., 2016). Studies such as these provide data for the implementation of groundwater protection policies where such policies are either weak or absent; however, challenges related to the lack of systematic monitoring and inconsistent land-use zoning have limited the ability to implement policies that are specific to the protection of karst aquifers. Few karst regions in the world have been more extensively studied and, more notably, dye-traced than in south-central Kentucky.

South-central Kentucky is a classic example of a well-developed karst landscape and includes the longest-known cave system, Mammoth Cave. Three physiographic regions comprise this area, including the Mammoth Cave Plateau, the Dripping Springs Escarpment, and the Pennyroyal Plateau, as well as the shallow, well-developed Mammoth Cave karst aquifer that formed in the Girkin, Ste. Genevieve, and St. Louis Limestones (Palmer, 1995). The once widely-accepted concept of "out of sight, out of mind," coupled with rapid recharge and discharge rates, historically led to the contamination of the Mammoth Cave aquifer via point-source pollution; specifically, the intentional, direct injection of waste into the subsurface.

[1]Department of Earth, Environmental, and Atmospheric Sciences, Western Kentucky University, Bowling Green, KY 42101
[2] current affiliation: Oklahoma Geological Survey, Sarkeys Energy Center, Norman OK 73019
* Corresponding author cesalea.osborne@gmail.com

Between 1975 and 1987, regional hydrogeologic investigations, including over 500 groundwater dye-traces, were conducted in the south-central Kentucky karst region to identify sources of contamination. Twenty-eight major groundwater basins were delineated in the Pennyroyal Plateau physiographic region during this time, including the Gorin Mill groundwater basin, one of the largest in south-central Kentucky, draining an area of 394 km^2 (Quinlan and Ewers, 1989; Meiman et al., 2001; Blair et al., 2012). The Gorin Mill groundwater basin drains two distinct subbasins that converge approximately eight kilometers northeast of the city of Horse Cave. The southwestern segment of this groundwater basin, known as the Hidden River groundwater subbasin, comprises over 80 % (324 km^2) of the Gorin Mill groundwater basin and includes Hidden River Cave (Fig. 1). The results of the hydrogeologic investigations determined that the most extensive contamination occurred within the Hidden River groundwater subbasin.

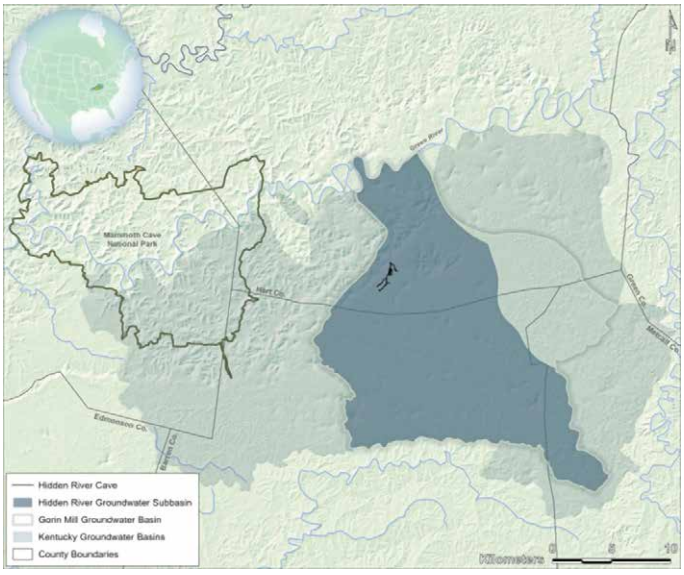

Figure 1. Groundwater basins in south-central Kentucky, including the Hidden River groundwater subbasin that makes up most of the larger Gorin Mill groundwater basin. Data from the Kentucky Division of Geographic Information (KDGI) (https://kygeonet.ky.gov) and the Kentucky Geological Survey (KGS) (http://www.uky.edu/KGS/gis).

The Hidden River groundwater subbasin is a transboundary basin that spans multiple counties in south-central Kentucky, including Barren, Hart, and Metcalfe counties, and includes L&N Cave (surveyed at 3 km) in Cave City, Hidden River Cave (16 km) in Horse Cave, and the Hidden River Complex (32 km) situated near the Green River, which have all been connected via groundwater dye-tracing. All serve as subsurface tributaries of the Hidden River groundwater subbasin and exhibit distributary flow; flooded, low-level conduits have created a system of interconnected passages where water flows north and resurges through 46 springs along the Green River, an important water resource on which several communities depend (Quinlan and Rowe, 1977). This study focused on Hidden River Cave due to its proximity to industrial development, its history of significant contamination, and its direct connection to the Mammoth Cave aquifer, which also serves as a water resource.

The entrance to Hidden River Cave is located in a 30 m deep collapse sinkhole that is owned and managed by the American Cave Museum (McGrain and Currens, 1978; Foster, 2009). High, interspersed breakdown rooms, large river passages, and floodwater mazes exist in the cave that recharge the Mammoth Cave aquifer and support myriad subsurface ecosystems (White et al., 1970; Quinlan and Ewers, 1989; Worthington et al., 2000).

Commercial development, along with point-source groundwater contamination, increased in Horse Cave during the 1970s. Pollutants were commonly injected into the subsurface through sinkholes and included raw sewage, heavy metals from a chrome plating plant, creamery waste, and oil refinery waste, among others. Based largely on the regional hydrogeologic investigations of Quinlan and Rowe (1977) and the Environmental Protection Agency (EPA, 1981), a new wastewater treatment facility was developed in 1989, which has significantly improved the water quality of Hidden River Cave. Additionally, the American Cave Conservation Association (ACCA) has established good working relationships with the industries that have directly impacted recharge to the cave system. Despite these changes in groundwater resource management, land-use boundaries in the city of Horse Cave intersect with areas of recharge that still introduce contaminants into the groundwater system.

This study used an integrative approach by combining groundwater dye-tracing, high-resolution stage data collection, and remote sensing analysis in a geographic information system (GIS) to assess land-use impacts on the hydrology of the Hidden River groundwater subbasin. Additionally, implications for U.S. federal, state, and local stormwater management regulations were reviewed, and suggestions were made to improve on these regulations to protect karst groundwater.

MATERIALS AND METHODS

Groundwater Dye-Tracing

Dye receptors were placed in Hidden River Cave at the East River, South River, areas in the Breakdown Canyon (i.e., the Breakdown Canyon entrance, Site 007, drainage wells), the Waterfall Room, and the headwaters of Wheet River (Fig. 2). The East River is the primary downstream tributary of Hidden River Cave and begins at the bottom of the cave's collapsed entrance, draining an area of ~150 km^2. The South River is a smaller tributary of the East River

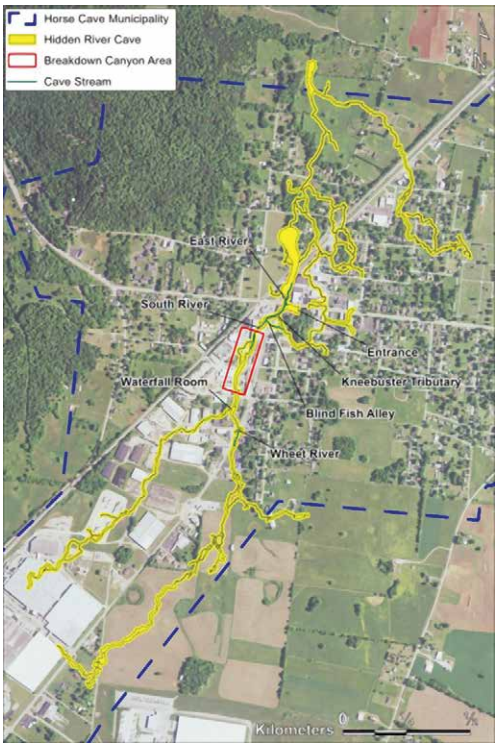

Figure 2. Hidden River Cave, Horse Cave, Kentucky. Data from the Cave Research Foundation and the KGS.

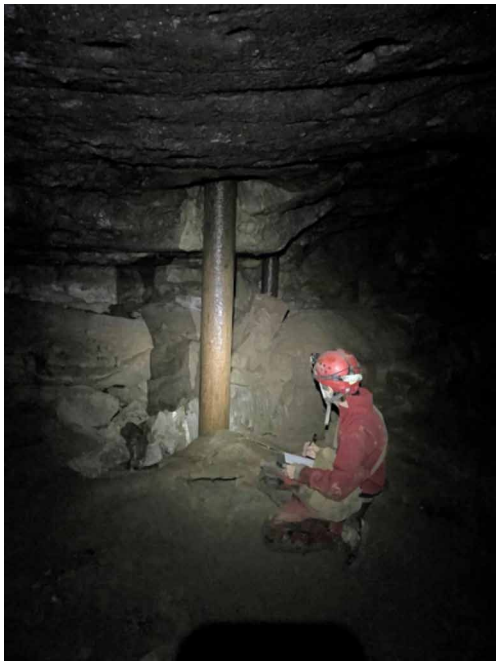

Figure 3. Drainage well casings in the Breakdown Canyon section of Hidden River Cave.

and drains an area of ~8 km^2 (Quinlan and Rowe, 1977). Wheet River is the primary upstream tributary of Hidden River Cave and is suggested to form the main tributary of the South River (Nims, P., 2018, pers. comm., July 13. Horse Cave, Ky.: ACM) several smaller tributaries and seeps are also suggested to be connected to the South River and recharged via sinkholes. Each of these sites exhibit background fluorescence characteristics similar to optical brighteners and fluorescein (Raedts and Smart, 2015), thus limiting the selection of dyes that can be used for tracing.

Poorly-drained depressions in the city of Horse Cave have been modified by the installation of drainage wells. Among these, two casings are visible in the Breakdown Canyon section of Hidden River Cave (Fig. 3), one of which is inferred to drain wastewater from a concrete mixing plant. This site exhibits the most notable source of contamination, where short-wavelength emitters that are typical of diesel fuels, lubricants, and soaps were observed in seeps and drips near the well casing. Additionally, recharge to the Waterfall Room consistently exhibits a very low, ambient fluorescein peak (515 nm) and produces a distinctive chlorine odor (Raedts and Smart, 2015).

Utilities (particularly stormwater) are not well-documented in Horse Cave, and the management of these features is not apparent (Raedts and Smart, 2015). Thus, four sites in Horse Cave were chosen for dye injection and georeferenced using Collector for ArcGIS (v. 19.0.2). These included a storm drain at the Horse Cave car wash (Fig. 4) that was suggested to discharge at the Waterfall Room (Nims, P., 2018, pers. comm., July 13. Horse Cave, Ky.: ACM), a drainage well located near the concrete mixing plant, and two storm drains near the now-retired Horse Cave Recycling Center. While several sinkholes within the municipality are suitable for dye-tracing, this study focused on infrastructure that has long been questioned by the ACCA.

Figure 4. Horse Cave car wash storm drain.

Each surface and subsurface site was photo-documented and given a unique inventory name and number (Table 1, Fig. 5). Two phases of groundwater dye-tracing occurred during this study; each receptor inventory number corresponds to its respective trace (i.e., the Waterfall Room (003) is denoted 003-1 for Phase I dye-tracing and 003-2 for Phase II dye-tracing).

Dye-Tracing Procedures

Background fluorescence monitoring occurred before each dye injection to detect dyes used in previous studies, pollutants, or natural compounds with fluorescence properties that may be similar to the dyes used by the Crawford Hydrology Laboratory (CHL) at Western Kentucky University. Dye receptors were installed in the main flow of each site and consisted of five-centimeter mesh bags filled with approximately three grams of activated coconut charcoal. Background monitoring occurred for one week

Table 1. Dye-tracing feature inventory.

Dye Injection Sites		Dye Receptor Locations	
Site ID	**Location**	**Site ID**	**Location**
DT1	Horse Cave Car Wash	001	Wheet River
DT2	Injection Well	002	Board Room
DT3	Recycling Center Storm Drain A	003	Waterfall Room
DT4	Recycling Center Storm Drain B	004	Well Casing A
...	...	005	Well Casing B
...	...	006	Well Casing C
...	...	007	Site 007
...	...	008	Breakdown Canyon
...	...	009	South River
...	...	010	East River

before each phase of dye-tracing, after which each dye receptor was rinsed in the respective cave stream to free the sample of any accumulated sediment, carefully placed into a clearly labeled, sealable plastic bag, and stored in a cooler to be transported to the CHL for analysis. New receptors replaced the background samples to prepare for the subsequent dye-traces.

In the laboratory, an eluent consisting of propanol, distilled water, and ammonium hydroxide prepared at a ratio of 5:3:2 was used to extract dye from one gram of charcoal from each dye receptor; the elutant was then analyzed using synchronous scanning on a Shimadzu RF-6000 spectrofluorophotometer following established CHL (2016) protocols. The emission spectra of the synchronous scans were plotted on a laser printer, and the results of the analysis were recorded in Excel.

Fluorescent dyes for each trace were chosen based on the analysis and interpretation of background fluorescence spectra. The quantity of dye for each injection was calculated via the following equation as per Aley and Fletcher (1976):

$$W_d = 1.478 \sqrt{\frac{dQ}{v}}, \quad (1)$$

where W_d represents the weight of the dye to be used (kg), d represents the distance between injection and receptor sites (km), Q represents discharge (m^3/s), and $\mathbf{u}$ represents stream velocity (m/s).

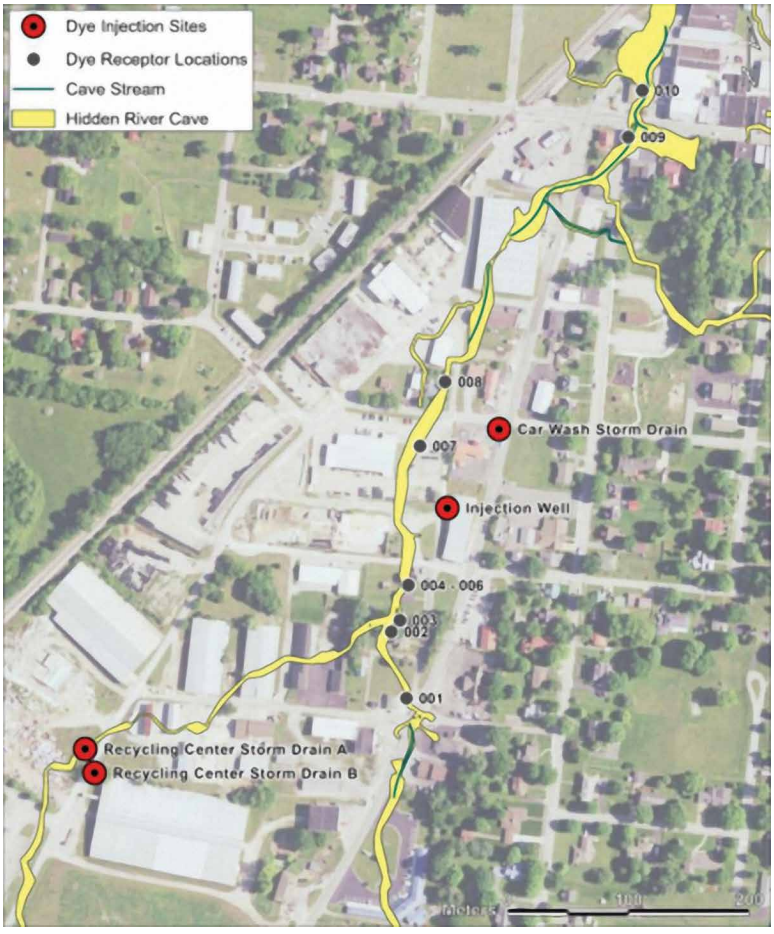

Figure 5. Dye receptor sites in Hidden River Cave and dye injection locations in Horse Cave. Data from the CRF and the KGS.

Dye injection occurred at four sites in the city of Horse Cave, and monitoring occurred for one to two weeks for each phase of dye tracing. After the monitoring period, the receptors were collected, stored, and transported to the laboratory for analysis following the CHL protocols.

Phase I Dye-Tracing

Phase I background monitoring occurred on March 9, 2018 and consisted of the placement of nine receptors at all but one site (007). The background receptors were retrieved on March 16, 2018, and a six-dye background analysis was conducted on March 20, 2018 against the standards Tinopal CBS-X (OB, FB351), Fluorescein (FL, AY73), Eosine (EO, AR87), D&C Red 28 (Phloxine B) (R28, AR92), Rhodamine WT (RWT, AR388), and Sulphorhodamine B (SRB, AR52).

Six sites exhibited positive background fluorescence, including the well casings, where OB, FL, R28, and RWT were detected. The Waterfall Room exhibited no significant background concentrations. Thus, RWT was chosen to trace the Horse Cave car wash storm drain (DT1) that was suggested to be associated with recharge to the Waterfall Room, and EO was chosen to trace the drainage well located near the concrete mixing plant (DT2). Phase I dye injection occurred during the evening of April 6, 2018 and included the injection of 0.5 kg of RWT into the car wash storm drain

and 0.3 kg of EO into the drainage well. Both dyes were injected before a rain event to ensure proper flushing. The dye receptors were retrieved on April 20, 2018 and analyzed on April 26, 2018 using CHL protocols.

Phase II Dye-Tracing

Phase II background monitoring consisted of the placement of 10 receptors on July 20, 2018, which included an additional site in the Breakdown Canyon section (007). The background receptors were retrieved on July 27, 2018, and a five-dye background analysis was conducted on August 1st using OB, FL, EO, RWT, and SRB standards.

Four dyes were detected in the background samples, including OB, FL, EO, and RWT. Based on these results and the previous use of EO and RWT, SRB was chosen to trace the Recycling Center Storm Drain A (DT3), and FL was chosen to trace Recycling Center Storm Drain B (DT4). Phase II dye injection occurred on August 3, 2018, and included 0.5 kg of SRB into Recycling Center Storm Drain A and 0.5 kg of FL into Recycling Center Storm Drain B. Both dyes were flushed using a fire truck provided by the Horse Cave fire chief. Dye receptors were retrieved on August 14th and analyzed on August 16th using the CHL protocols.

CHARACTERIZATION OF STREAM STAGE

Two Onset HOBO pressure transducers (model U20L-02) were installed in Hidden River Cave on June 10, 2018, to collect high-resolution stage data after flooding events occurred that limited accessibility to Hidden River Cave. The transducers were installed in PVC stilling wells near the Kneebuster tributary in the South River and at the Thomas Boardwalk in the East River to characterize stream responses to precipitation events until September 29, 2018. Each sonde collected five-minute resolution water-level data, except when briefly pulled to download the data; due to an error in deployment, the East River sonde excludes data from Julian dates 180 to 201. The stage data were processed using Onset HOBOware Pro (v. 3.7.15), which incorporated water level reference readings and barometric pressure compensation data that were recorded at the time of each data download. The processed stage data were organized in Excel, graphed using SigmaPlot (v. 11.0), and compared to five-minute precipitation data acquired from the Kentucky Mesonet HDYV monitoring station located in Munfordville (https://www.kymesonet.org/).

LAND-USE OVER THE HIDDEN RIVER GROUNDWATER SUBBASIN

Changes in land-use over the Hidden River groundwater subbasin between 1989 and 2017 were determined using supervised classification in ArcGIS Pro (v. 2.2) and 30 × 30 m Landsat 5 (10/22/1989) and Landsat 8 (09/26/2017) multispectral imagery obtained from the United States Geological Survey (USGS) Global Visualization Viewer (GloVis) (https://glovis.usgs.gov). The scope of the land-use analysis was broadened to include the entire Hidden River groundwater subbasin, as changing land-use in other areas of the subbasin could negatively impact overall recharge. Additionally, because most of Hart County's industry is located in Horse Cave (HCCC, 2013), this time frame was chosen based on the 28-year gap that exists between the publications of the respective City of Horse Cave zoning ordinances.

The study area included a feature class of the Gorin Mill groundwater basin collected from the Kentucky Geological Survey (KGS) that was modified to represent the associated Hidden River groundwater subbasin according to the extent defined by Ray and Currens (1998). Using the Hidden River groundwater subbasin feature class and the Clip tool in ArcGIS Pro, both images from GloVis were clipped to the subbasin boundaries. A qualitative analysis comparing the 1989 and 2017 imagery was conducted during supervised classification, which included creating training samples, reclassifying the imagery, and performing post-classification processing on both images. The results of the reclassification were then compared quantitatively by determining the percentage of land-use classes for each image and an assessment was conducted to determine the accuracy of the classification method used.

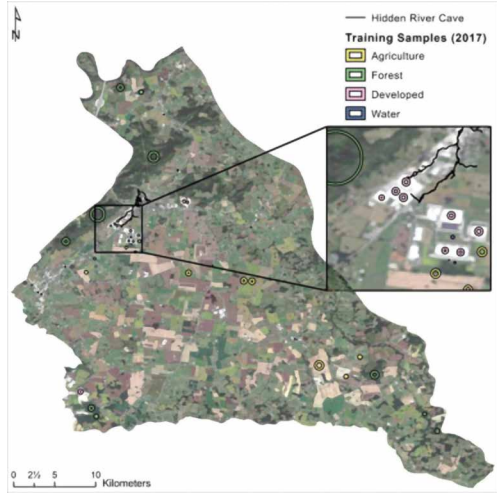

Figure 6. Example of training samples created from the 2017 Landsat 8 imagery used to perform supervised classification. Data from GloVis and the USGS 2011 NLCD (https://www.usgs.gov/centers/eros/science/national-land-cover-database).

Supervised classification was conducted for each image using the Classification Wizard in ArcGIS Pro, and training samples (Fig. 6) were created using the Training Samples Manager and schema provided by the USGS 2011 National Land Cover Dataset (NLCD), which includes the following land-use classes: (1) water, (2) developed, (3) forest, and (4) agriculture. Reclassified rasters were generated from the training samples. Post-classification processing was then applied to the reclassified images by using generalization tools, which remove the noise that is created by isolated pixels or small, misclassified regions and automates the assignment of more reliable values; the Majority Filter tool removed isolated pixels from the reclassified raster, and the Boundary Clean tool smoothed the

class boundary edges and grouped the classes to produce more organized imagery (Keranen and Kolvoord, 2014).

To determine the percentages of land cover types, a new field named Percent was added to the attribute table of each reclassified raster and populated via the Field Calculator tool; for each land-use category, the total number of pixels in the respective reclassified image (determined using the Summary Statistics tool) was divided by the number of pixels representing that category and multiplied by 100. These data were used to assess the approximate percentages of land-use change over the Hidden River groundwater subbasin between 1989 and 2017.

Accuracy Assessment of Supervised Classification

To determine the accuracy of the performed supervised classification, the errors of omission (features that have been excluded from the reclassified imagery that exist) and commission (features that do not exist that have been included in the reclassified imagery) were calculated by generating an error matrix from ground-truthed data, which compares the organized, reclassified imagery to higher resolution aerial imagery (Keranen and Kolvoord, 2014).

Twenty-five points were randomly generated for each image using the Create Random Points tool. Because the reclassified image resolution is 30 × 30 m, a 30-meter buffer was created around the random points to represent the approximate area that a single pixel spans (Fig. 7). The reclassified imagery was then compared to 2016 Kentucky statewide 0.5 m aerial imagery that was downloaded from the Kentucky Division of Geographic Information to ground-truth land cover within the buffer boundaries. Note that high-resolution 1989 imagery was not available; thus, generalizations were made by analyzing the Landsat 5 multispectral imagery in conjunction with the 2016 Kentucky statewide 0.5 m aerial imagery.

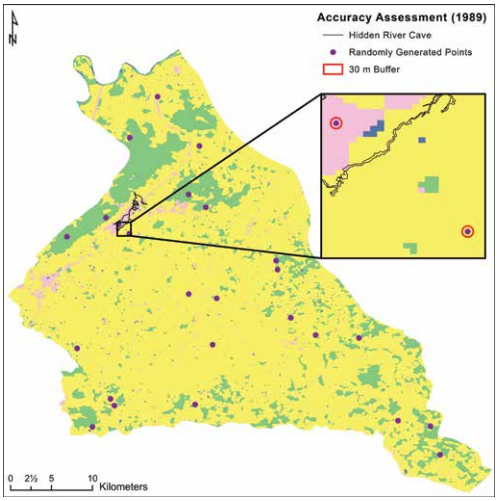

Figure 7. Example of random point generation; a 30 m buffer was created around each point to ground-truth the land cover type within the buffer. Data from GloVis and the USGS 2011 NLCD.

A new field was added to the random point feature class called GT (ground-truth) to record the correct type of land-use within the buffer according to the high-resolution imagery. Upon completion of ground-truthing, the Extract Values to Points tool was used on each of the reclassified images, which extracted the land-use values that the random points represented and added them to the attribute table of the Random Point feature class. The final attribute table included the ground-truthed values and the values determined by supervised classification, which were compared to determine the accuracy of the classification method used. An error matrix was constructed using the Select by Attributes tool to identify matching classifications. For example, to determine the number of points that were classified as water (1), the following query was used:

"GT 2017" = 1 AND "Supervised 2017" = 1

The same query was used to determine each corresponding land-use type for both images. From these data, the total classification accuracy percentages were calculated to determine the errors of omission and commission.

RESULTS AND DISCUSSION

Phase I and II Dye-tracing

During Phase I dye-tracing, it was anticipated that EO would discharge from drips and seeps surrounding Well Casing B (005-1) due to the suspected age and potential degradation of the well casing and that RWT would discharge at the Waterfall Room (003-1). Conversely, a high concentration of EO was detected at the Waterfall Room rather than RWT (Table 2); EO appeared to bypass the well casings and was detected again at the Breakdown Canyon entrance (008-1), the South River (009-1), and the East River (010-1). No dye was recovered at Well Casing B and, although a direct connection cannot be confirmed, a higher concentration of dye was detected at Well Casing A (004-1) than what the results of background fluorescence analysis determined. Further, the peak center associated with Well Casing A is more indicative of R28 than the recovery of RWT from the Horse Cave car wash storm drain (DT1); thus, 004-1 was considered a questionable positive. Like EO, a significant concentration of RWT was ultimately detected at the Breakdown Canyon entrance and beyond.

Because consideration was not made of RWT potentially being detected at the well casings, and the peak center for RWT and R28 are relatively similar, another trace should be conducted at the drainage well located near the concrete mixing plant (DT2) using a different dye, such as SRB. Alternatively, radiolocation can be used to determine the precise location of the well casing in relation to the surface, as few data exist regarding its installation and ownership (KGS, 1997). It is possible that the well casing seen on the surface is unrelated to either of those seen in the subsurface.

Table 2. Results of Phase I dye-tracing.

	Eosine			Rhodamine WT		
Feature ID	**Result[a]**	**Conc., ppb**	**Peak Ctr., nm**	**Result[a]**	**Conc., ppb**	**Peak Ctr., nm**
Waterfall Room (003-1)	+++	222.266	542.2	···	···	···
Well Casing A (004-1)	···	···	···	?+	5.828	564.6
Breakdown Canyon (008-1)	+++	14.962	542.2	++	8.290	568.4
South River (009-1)	+++	9.172	542.4	++	6.020	568.2
East River (010-1)	++	0.692	542.2	+	0.258	567.4

[a] + = Positive (10 times background or lowest detection limit)
++ = Very positive (100 times background or lowest detection limit)
+++ = Extremely positive (1,000 times background or lowest detection limit)
?+ = Questionable Positive

This inference is based on the misalignment of the GPS data used to georeference the well casing with respect to the approximate locations of the casings in the cave (Osborne, 2018). Therefore, future investigations should consider collecting high-accuracy GPS data and georeferencing the cave to confirm its locational accuracy.

It is unknown where the dyes used for Phase I tracing discharged from their respective injection sites or where water is flowing between the Waterfall Room (003) and the Breakdown Canyon entrance (008). An orange tint was detected at a pool in the Kneebuster tributary (Nims, P., 2018, pers. comm., July 13. Horse Cave, Ky.: ACM), which was not included in the dye-tracing procedures herein. This observation, however, is not surprising, as a small, neighboring tributary exists that connects the headwaters of the South River and the Kneebuster passage, known as Blind Fish Alley (Fig. 2). Concentrated RWT was also observed by the American Cave Museum (ACM) staff at Site 007; however, because the passage was unknown to the author before Phase I dye-tracing, a receptor was not placed there. This red pool, as well as an orange tint to the cascade in the Waterfall Room, was observed less than one day after Phase I dye injection took place (Russell, G., 2018. Pers. comm., May 2. Horse Cave, Ky.: ACM.)

In Phase II dye-tracing, FL and SRB were only detected at the South River (009-2) and the East River (010-2) (Table 3). A much higher concentration of each dye was detected at the South River site. Based on these results, other, concealed groundwater flow paths likely exist beneath the Breakdown Canyon section or in tributaries that lie outside of the known cave boundaries that ultimately discharge to the South River. The South River also could have been an outlet for more dye, either because it is a more direct route from the injection location, it experienced more flow during the monitoring period, or because the flow patterns at the South River where the receptor was deployed were ideal (or a combination of these possibilities). It is also possible that the East River headwaters effectively diluted the dye traveling from 009-2 to 010-2, resulting in lower dye concentrations.

The results of background fluorescence analyses conducted by Raedts and Smart (2015) determined that some tributaries in the cave exhibited consistent spectra. Indeed, the spectra seen during this study from sites such as Wheet River, the Waterfall Room, and the South and East Rivers align with their results. Several other sites in the city of Horse Cave (i.e., the Horse Cave laundromat, sinkholes, catchment basins, etc.) and Hidden River Cave (i.e., the Kneebuster tributary and upstream East River) should be the focus of future dye-tracing investigations. In-cave dye-tracing should also occur to confirm the implied connections between sites such as Wheet River, the Breakdown Canyon entrance, and the South River. Further, using the Hydrology toolset in ArcGIS Pro, the collective dye-traces conducted within the Hidden River groundwater subbasin could be modeled to develop more accurate, rather than inferred, groundwater flow paths. An interactive, visual model can provide a relatively simple way for the ACM to further convey to the public the importance of groundwater protection in karst regions.

The dye-tracing conducted herein also supported Raedts and Smart's (2015) suggestion that acute, point-source contamination events are linked to land-use practices in Horse Cave, as all dyes were detected in Hidden River Cave (Fig. 8). While qualitative dye-tracing does not provide the parameters that are necessary to determine the time of travel of recharge from drainage features on the surface to the cave, it does establish benchmark data that can be coupled

Table 3. Results of Phase II dye-tracing.

	Fluorescein			Sulphorhodamine B		
Feature ID	**Result[a]**	**Conc., ppb**	**Peak Ctr., nm**	**Result[a]**	**Conc., ppb**	**Peak Ctr., nm**
South River (009-2)	+++	277.419	518.4	+++	23.556	579.4
East River (010-2)	++	3.907	517.4	++	1.484	578.0

[a] ++ = Very positive (100 times background or lowest detection limit)
+++ = Extremely positive (1,000 times background or lowest detection limit)

with stream stage analyses to generalize the seemingly abrupt nature of recharge based on the aforementioned observations made by the ACM staff.

Characterization of Stream Stage

This study establishes the first recorded, high-resolution flow conditions in Hidden River Cave, which are critical for assessing the rate at which contaminants may enter the cave system. Cave stream responsiveness to four major precipitation events was analyzed using five-minute resolution precipitation data acquired from the Kentucky Mesonet HDYV monitoring station in Munfordville. Scattered thunderstorm events occurred from Julian date (JD) 176 to JD 179 and produced the highest rainfall values during this study (Fig. 9). The approximate baselevel conditions (determined by average minimum stage values) were met on JD 182 (three days after the final precipitation event). A series of four precipitation events occurred from JD 228 to JD 233 that caused subsequent peaks in each stream; a steady decline in stage occurred over nearly a week, although neither stream achieved baselevel conditions. Stage response from Tropical Storm Gordon (https://www.weather.gov/mob/gordon) is evident from JD 251 to JD 252. Water levels returned to near baseflow conditions on JD 256, four days after precipitation ended. The most significant storm event during this study occurred during the fall season's first major cold front, which brought rainfall from JD 264 to JD 267. Return to baseflow was not determined for this event due to time constraints. Overall, the East River produced higher stage values than the South River.

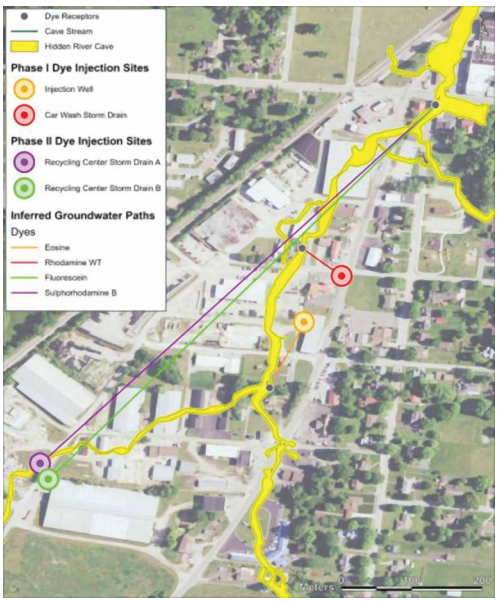

Figure 8. Inferred groundwater flow paths determined by Phase I and II dye-tracing. Data from CRF and KGS.

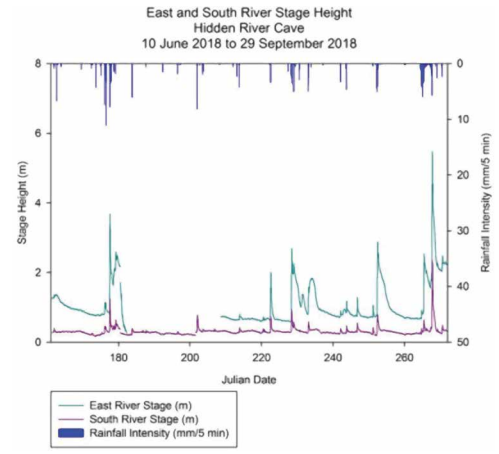

Figure 9. South River and East River stage responses to precipitation from June 10 to September 29, 2018. Data analyzed in SigmaPlot (11.0).

The flashy nature of the streams exhibited in the hydrograph is indicative of low storage, high transmissivity, and rapid drainage (Murdoch et al., 2016). Although this study occurred over a short period, the HOBO pressure transducers that were installed at the South and East Rivers provide important data to assess cave stream responsiveness to precipitation events to identify possible contaminant transport scenarios and for flood prediction.

Stage at the South River appeared to respond to precipitation events (and recede) more quickly than at the East River. Significant peaks in the East River hydrograph occur approximately thirty minutes after peak flow occurs at the South River; however, when the East River experienced recharge from sustained precipitation, response times were similar to those observed in the South River. Except for antecedent precipitation, the South River responds within 40 minutes to one hour, while the East River takes longer (approximately 1-1.5 hours). Additionally, except for sustained precipitation (i.e., from JD 228 to JD 233), it appears to take three to four days for both streams to recede to baselevel conditions after precipitation events end. Baselevel conditions were not met for the precipitation events that occurred from JD 228 to JD 233 before precipitation began again upon the arrival of Tropical Storm Gordon, although water recession occurred over nearly a week, aligning with Fiorillo's (2016) suggestion that hydrograph recession can occur over several days. These differing response times are likely indicative of the streams' respective catchment sizes, variations in matrix permeability and porosity (i.e., diffuse vs. conduit flow), storage, or karstification of the cave system (or a combination of these), as well as either inactive tributaries during low flow or the diversion of flow via increased discharge during precipitation events.

The stage data herein can serve as a benchmark to supplement future high-resolution hydrologic studies in Hidden River Cave. Future investigations should consider discharge at the South and East Rivers, as well as Wheet River, the Waterfall Room (where a funnel system, as exemplified by Groves et al. (2013), could be constructed), and the Breakdown Canyon entrance. Discharge data, coupled with in-cave dye-tracing that was previously suggested, can characterize the differences in volumetric flow between Wheet River, the Breakdown Canyon entrance, and the South River, as they are inferred to be hydrologically connected to one another. Additionally, discharge data coupled with quantitative dye-tracing can provide details about the fate and transport of contaminants (Li et al., 2016; Murdoch et al., 2016; Jiang et al., 2018), and hydrochemical analyses can be used to characterize the epikarst in Hidden River Cave and systematically monitor groundwater quality (Ryan and Meiman, 1996; Groves et al., 2013; Knierim et al., 2015;

Schreiber et al., 2015), parameters that have not yet been examined. Thus, it is important to understand the type and extent of infrastructural land-use over the Hidden River groundwater basin, as the impermeable nature of development often increases runoff and, consequently, contaminant transport in tributary catchments (Jiang et al., 2018).

Land-use over the Hidden River Groundwater Subbasin

Hidden River Cave is a case study example of the complexity of the relationship between urban land-use and recharge areas, such as those demonstrated by the dye-tracing herein. Thus, the entire Hidden River groundwater subbasin was examined to assess regional land-use that may further impact the groundwater system outside the main developed area of Horse Cave. Except for agricultural areas, all land-use types over the Hidden River groundwater subbasin have increased since 1989. Developed areas are arguably the most important to analyze for the purposes of this study, as they directly affect Hidden River Cave, according to the dye-tracing results herein. Supervised classification determined that development over the Hidden River groundwater subbasin increased by 7 % between 1989 and 2017 (Fig. 10). While developed areas do not make up the dominant land-cover type, they are critical to understand based on the history of groundwater contamination in this region and the current, discrete contamination events that have occurred since remediation began in 1989.

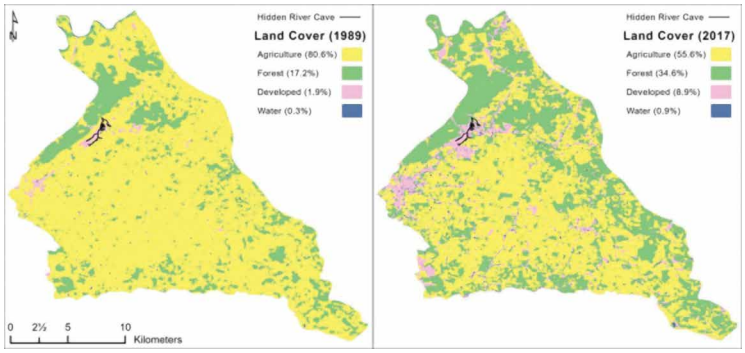

Figure 10. Comparison of the reclassified 1989 and 2017 aerial imagery. Data from GloVis, USGS 2011 NLCD, CRF, and KDGI.

While agricultural areas decreased by 25 % since 1989, forested areas increased by 17.7 %. It is possible that more agricultural land was converted to forest after several events, such as abandonment, ownership conversion, or restoration efforts. A 0.6 % increase in water can also be seen; however, several discrepancies exist between land-use types, which can be attributed to the lower resolution (30 × 30 m) imagery. For example, water bodies tend to appear either varying shades of green or brown and therefore contain similar reflectance values as agricultural, forested, and industrial areas (as some industrial buildings have green roofs). In the reclassified 2017 imagery, water appears to surround developed areas in Horse Cave; future land-use investigations should consider the occurrence of sinkholes and the amount of precipitation the study area received during the time imagery was taken, as well as the development of catchment basins, such as Creacy Lake.

Using U.S. Census data, population changes over time could shed light on the potentially increased stress that may be imposed on the utilities in Horse Cave (Knierim et al., 2015; Denizman, 2018). Specifically, sewage utilities and the percentage of the population that relies on septic systems should be assessed, as Raedts and Smart (2015) discovered sections of the cave that exhibited fluorescence peaks characteristic of optical brighteners found in raw sewage. Additionally, many rural parts of Kentucky are home to concentrated animal feeding operations (CAFOs), which commonly are not considered risks to karst groundwater (Brahana et al., 2014; Knierim et al., 2015; Murdoch et al., 2016; Tagne and Dowling, 2018). Thus, CAFOs and other agricultural enterprises in Hart County should be included in future land-use analyses.

Accuracy Assessment of Supervised Classification

An accuracy assessment was conducted by comparing the results of the reclassified 1989 Landsat 5 TM and the 2017 Landsat 8 aerial imagery to ground-truthed data using 2016 Kentucky state wide 0.5 m aerial imagery. Overall accuracy was calculated by dividing the number of correct pixels in the error matrix (the sum of the diagonal) by the total number of pixels. Additionally, the errors of commission (column total) and omission (row total) were calculated by dividing the number of correct pixels in a land-use category by the total number of pixels in that category (Tables 4 and 5).

Results revealed that the reclassified 1989 aerial imagery produced a slightly lower accuracy than the results of the 2017 imagery when compared to ground-truthed data, although these percentages reflect that the supervised classification conducted herein produced relatively accurate results. It is important to note, however, that the classification method used does not account for all of the infrastructure within the study area. For example, the road that dissects the study area consists of pixels that represent all types of land-use rather than a solely developed feature. Thus, these percentages do not reflect all development, but they differ enough to conclude that development has increased.

Developed areas can significantly modify the natural processes of subsurface recharge via features such as impermeable surfaces (i.e., parking lots and landfills) and utility networks (Zhou, 2007). Modern construction typically includes extensive paving over the natural soil surface, which can effectively decrease local recharge by lessening percolation areas while simultaneously increasing the amount of surface runoff to otherwise relatively inactive parts

Table 4. Accuracy assessment of the reclassified 1989 Landsat 5 TM imagery.

	Actual Category: Ground-Truth					Error of
Classified Category	Water	Developed	Forest	Agriculture	Total	Commission, %
Water	0	0	0	0	0	0
Developed	0	1	0	0	1	100
Forest	0	0	6	0	6	100
Agriculture	1	0	3	14	18	77.7
Total	1	1	9	14	25	···
Error of Omission, %	0	100	66.7	100	···	···
Overall Accuracy, %	84	···	···	···	···	···

Note: errors of commission (column total) and omission (row total) were calculated by dividing the number of correct pixels in a land-use category by the total number of pixels in that category and multiplying the quotient by 100 to obtain a percentage. Overall accuracy was calculated by dividing the number of correct pixels in the error matrix (the sum of the diagonal) by the total number of pixels.

Table 5. Accuracy assessment of the reclassified 2017 Landsat 8 imagery.

	Actual Category: Ground-Truth					Error of
Classified Category	Water	Developed	Forest	Agriculture	Total	Commission, %
Water	1	0	0	0	1	100
Developed	0	4	0	0	3	100
Forest	0	0	7	3	11	63.6
Agriculture	0	0	0	10	10	100
Total	1	4	7	13	25	···
Error of Omission, %	100	100	100	76.9	···	···
Overall Accuracy, %	88	···	···	···	···	···

Note: errors of commission (column total) and omission (row total) were calculated by dividing the number of correct pixels in a land-use category by the total number of pixels in that category and multiplying the quotient by 100 to obtain a percentage. Overall accuracy was calculated by dividing the number of correct pixels in the error matrix (the sum of the diagonal) by the total number of pixels.

of the groundwater system (Jiang et al., 2018). Indeed, most of the explored cave system is covered by development (Fig. 10), the impervious nature of which has likely altered the natural recharge and discharge mechanics of the Hidden River groundwater subbasin. Further, stormwater discharge from development sites does not appear to be effectively regulated in Hart County. Thus, the suggested potential for mitigating further contamination of the Hidden River groundwater subbasin through the techniques used in this research can be supplemented by examining the existing policies regarding stormwater discharge regulations in karst regions at national, state, and local levels.

Implications for Karst Stormwater Regulations

Numerous studies exist that provide the scientific basis to support the need for improved groundwater management in transboundary karst regions (Marín et al., 2000; Escolero, 2002; Bauer-Gottwein et al., 2011; Christenson et al., 2011; Nedvidek, 2014; Ravbar and Šebela, 2015; Stevanović et al., 2016; Castro, 2017; Turpaud et al., 2018). A prevalent theme, however, is the lack of the implementation of such practices (Fleury, 2009; Richardson, 2018).

Except for the management of federally-owned land, where laws such as the Endangered Species Act (1973) and the Federal Cave Resources Protection Act (1988) indirectly protect karst resources, the U.S. federal government is limited in its authority to address concerns related to groundwater quality in karst regions. For example, the Clean Water Act (1972), including the National Pollutant Discharge Elimination System (NPDES) permit program, only protects against the contamination of surface waters (EPA, 2019), and the Safe Drinking Water Act (1974) mentions groundwater but regulates only those karst areas that contain sole-source aquifers (Nedvidek, 2014; Richardson, 2018). Rather, state governments and, to the extent granted by the state, local governments hold the primary authority to regulate groundwater, although this is often not conducted in a meaningful way (Fleury, 2009).

In Kentucky, policies regarding stormwater discharge are contained in Title 401, Chapter 5 of the Kentucky Administrative Regulations (KGA, 2020). The Kentucky Pollutant Discharge Elimination System (KPDES), the state-administered version of the NPDES, requires operators to obtain a permit and create a Stormwater Pollution Prevention Plan (SWPPP) for proposed development. The KPDES implements the six Minimum Control Measures (MCMs) outlined in

Phase II (1998) of the federal NPDES permit program (EPA, 2018) but fails to address regulations that are specific to the karst landscape that makes the state unique. These six MCMs rely heavily on education and quality BMP development. Indeed, a plethora of educational resources and public outreach programs exist in Kentucky that reiterate the importance of protecting karst waters; however, relying solely on education and BMPs (the effectiveness of which are rarely measured) dismisses the opportunity to collect quantitative data from the systematic groundwater monitoring that is necessary for the protection of karst waters (Taylor et al., 2007; Nedvidek, 2014).

In the Hart County Comprehensive Plan, recognition of the karst topography of Hart County and adequate stormwater drainage for development projects is included under the Land Use and Development Objectives (HCPC, 2020, p. 14); however, a foundational management plan is not provided to reinforce these objectives. More specifically, stormwater management is addressed in Articles 10 and 18 of the Hart County Planning Commission's Subdivision Regulations (HCPC, 2007). Similar to the state's SWPPP, the Hart County Planning Commission requires a Storm Water Management Plan (SWMP) for development; here, sinkholes, the only mention of a karst-related feature, are required to be identified, but no formal structure exists for regulating stormwater discharge to these features.

As aforementioned, the City of Horse Cave Zoning Ordinance (CoHC, 2017) which adheres to and references the Hart County Planning Commission's Subdivision Regulations, had not been updated from 1989 (CoHC, 1989) until 2017. Few improvements have been made since 1989; similar to the subdivision regulations, the impacts that development may have on groundwater are not addressed or properly mitigated. Further, all three documents briefly mention karst in the form of regulating development near sinkholes. Setbacks are required around sinkholes, as they "shall be preserved in their natural state to provide drainage to the surrounding area" (HCPC, 2007, p. 41); yet, there is no requirement for monitoring said drainage.

Perhaps the most significant improvement to the 2017 City Zoning Ordinance is the associated map that was created by the Barren River Area Development District using ArcGIS Online (BRADD, 2017). This map provides significant detail compared to that of the 1989 zoning ordinance, but the fact that it was not created by either Hart County or the City of Horse Cave emphasizes their need for GIS. County or city employees can adopt GIS practices using either open-source (i.e., QGIS) or closed-source (i.e., Esri) GIS software, where an inventory of utilities and drainage wells could be developed. Collaboration with GIS software providers can also implement free or relatively inexpensive software training to build and upkeep such an inventory. Additionally, the option to download open-source data from local, state, and federal organizations provides a unique opportunity to complete various cost-effective, broad-scale analyses in GIS (Wilson and Rocha, 2016).

The City of Bowling Green, Kentucky, in collaboration with Western Kentucky University, has developed an inventory of stormwater drainage features that are maintained in a GIS, and they have effectively raised the bar in terms of establishing an efficient stormwater monitoring program (https://www.underbgky.org/). Nedvidek (2014) explained that city officials in Bowling Green are aware of the importance of these data for establishing broad-scale permit compliance and producing benchmark data to implement regulations regarding stormwater discharge to karst groundwater. A partnership such as this between the City of Horse Cave and the ACCA could establish an agenda to systematically monitor stormwater discharge to groundwater, especially since the ACCA has existing partnerships with institutions that provide grant opportunities for research (i.e., the Cleveland Grotto, Western Kentucky University, the University of Western Ontario, McMaster's University, etc.). Additionally, Horse Cave's proximity to Mammoth Cave National Park and the City of Bowling Green provides avenues for further collaboration.

Several studies have produced benchmark data that suggests the need for improved management of the Hidden River groundwater subbasin (Quinlan and Rowe, 1977; Quinlan and Ewers, 1989; Lewis, 1995; Raedts and Smart, 2015; Broderick et al., 2017; Osborne, 2018; Feist et al., 2020). The following recommendations, based on the results of the analyses herein, can also be used to further protect the Hidden River groundwater subbasin.

- Hart County and/or the cities within Hart County should consider implementing an organizational GIS using either open-source or closed-source GIS software, and training services should be provided to employees for the creation and maintenance of a geodatabase containing a detailed inventory of utilities, wells, and karst features;
    - Benchmark data from local studies should be synthesized and, where applicable, added to a geodatabase;
    - Exploration and data collection should continue at L&N Cave and the Hidden River Complex;
- The City of Horse Cave zoning ordinance should be regularly revised (i.e., annually or bi-annually) and should consider the local geology, including the maturity of the Pennyroyal Plateau, to make more informed decisions regarding development;
- The City of Horse Cave should form partnerships with the ACCA, Mammoth Cave National Park, nearby municipalities (i.e., Bowling Green, Park City, Cave City, etc.), universities, and caving organizations to establish and enforce more effective regulations regarding stormwater discharge to groundwater;

- Planning and development documents in Hart County should include stormwater discharge policies that are specific to the protection of karst groundwater;
    - Stormwater discharge regulations in Hart County should surpass those established by the KPDES;
    - The regional karst groundwater basins and their respective subbasins should be acknowledged by the officials that create and enforce development ordinances and by development operators;
    - SWMPs should require systematic water quality monitoring (i.e., greater than quarterly) at discharge areas such as Gorin Mill Spring to measure the performance of BMPs set forth by the site operator.

CONCLUSIONS

An integrative approach, which can be applied to other transboundary karst regions, combined groundwater dye-tracing, high-resolution stage data collection, and remote sensing analysis in a GIS to assess land-use impacts on the hydrology of the Hidden River groundwater subbasin.

Groundwater dye-tracing confirmed that stormwater infrastructure in Horse Cave discharges to Hidden River Cave and, subsequently, to the Hidden River groundwater subbasin, as each of the dyes used during this study were recovered. High-resolution stage data determined that the major trunk streams of Hidden River Cave respond to precipitation events approximately 40 minutes to 1.5 hours after they begin; except for sustained precipitation, baselevel conditions are reached three to four days after precipitation ends. These data and the aforementioned observations of dye made by the ACM staff less than one day after dye injection occurred imply that recharge to Hidden River Cave is relatively abrupt. Thus, the rate at which contaminants enter and traverse the subsurface is likely also abrupt.

Supervised classification in ArcGIS Pro using 30 × 30 m multispectral imagery from the USGS characterized changes in land-use over the Hidden River groundwater subbasin from 1989 to 2017. Development is largely concentrated in Horse Cave and has increased by approximately 7 % between 1989 and 2017, suggesting an increase in impervious surfaces, which can significantly alter the natural recharge and discharge mechanics of the subbasin and introduce a higher volume of contaminants. Additionally, weaknesses were identified in the current stormwater management regulations at the U.S. federal, state, and local levels, where the sparsity or absence of karst-specific regulations suggests either the improvement or implementation of such regulations.

Hidden River Cave serves as an important economic and cultural resource for Horse Cave and the wider region. This research supplements prior studies and addresses gaps in the literature by evaluating land-use and recharge relationships at a local, rather than regional, scale, as most of the commercial development within the boundaries of the Hidden River groundwater subbasin lies over Hidden River Cave. It also demonstrates the important contribution of localized groundwater investigations to broader karst management and sustainable development planning, including for policy development toward water resource protection.

ACKNOWLEDGMENTS

This work was supported by the Graduate Student Research Committee at Western Kentucky University under Grant number 221531 and the Cleveland Grotto Science Fund. Special thanks to Dave Foster for allowing me to conduct research freely in Hidden River Cave, to the staff at the American Cave Museum and my friends Peggy, Steve, and Chelsea, whose knowledge of the cave contributed greatly to this work, and to the Horse Cave fire chief for flushing my dye during the peak of summer. The research herein is very dear to me, and it is my hope that future generations will continue to work toward creating a pristine environment for Hidden River Cave. Not only does this research support the goals of the American Cave Conservation Association, but also the overall conservation and preservation of karst landscapes.

This work is dedicated to J.F. Quinlan – his work in the south-central Kentucky karst region was phenomenal, and his legacy continues through this research.

REFERENCES

Aley, T., and Fletcher, M.W., 1976, The Water Tracer's Cookbook: Missouri Speleology, v. 16, no. 6, p. 1−32.

Bauer-Gottwein, P., Gondwe, B.R.N., Charvet, G., Marín, L.E., Rebolledo-Vieyra, M., and Merediz-Alonso, G., 2011, The Yucatán Peninsula Karst Aquifer, Mexico: Hydrogeology Journal, v. 19, no. 3, p. 507−524, https://doi.org/10.1007/s10040-010-0699-5.

Blair, R.J., Ray, J.A., O'dell, P.W., Marbert, B.S., and Goodmann, P.T., 2012, Integrated surface water and groundwater assessment of large springs in the Green River Basin (BMU4, Round 2), Kentucky Division of Water: https://eec.ky.gov/Environmental-Protection/Water/Reports/Reports/NPS0503-BMU4R2.pdf, [accessed Dec. 20, 2017].

BRADD (Barren River Area Development District), 2017, Horse Cave Zoning Information; https://bradd-ky.maps.arcgis.com/apps/Information-Lookup/index.html?appid=5e263aca436c4e3699a02a9f3cce0ec9, [accessed Oct. 24, 2018].

Brahana, V., Nix, J., Bitting, C., Bitting, C., Quick, R., Murdoch, J., Roland, V., West, A., Robertson, S., Scarsdale, G., and North, V., 2014, CAFOs on Karst – Meaningful data collection to adequately define environmental risk, with a specific application from the Southern Ozarks of Northern Arkansas: U.S. Geological Survey, Scientific Investigations Report 5035, 10 p.

Broderick, C.A., Wicks, C.M., and Paylor, R.L., 2017, Testing the effectiveness of beryllium-7 as a tracer of the movement of sediment over short periods along a cave stream in Hidden River Cave, Kentucky U.S.A.: Journal of Cave and Karst Studies, v. 79, no. 2, p. 84−88, https://doi.org/10.4311/2016ES0115.

Castro, R.B.P., 2017, Statistical analysis of karst aquifer pollution, Karst Flow Model validation at laboratory scale, and development of seepage meter: [Ph.D. dissertation]: Tallahassee, Florida State University, 101 p.

CHL (Crawford Hydrology Laboratory), 2016, Standard Operating Procedures: Bowling Green, Crawford Hydrology Laboratory, 80 p.

Christenson, S., Osborn, N.I., Neel, C.R., Faith, J.R., Blome, C.D., Puckette, J., and Pantea, M.P., 2011, Hydrogeology and Simulation of Groundwater Flow in the Arbuckle-Simpson Aquifer, South-Central Oklahoma: U.S. Geological Survey, Scientific Investigations Report 2011-5029, 104 p., https://doi.org/10.3133/sir20115029.

CoHC (City of Horse Cave), 1989, Zoning Ordinance: City of Horse Cave, Kentucky, https://www.horsecaveky.com/Zoning%20Ordinance-1.pdf, [accessed Oct. 24, 2018].

CoHC (City of Horse Cave), 2017, 2017 City Zoning Ordinance: https://www.horsecaveky.com/Zoning%20Ordinance-2017-1.pdf, [accessed Oct. 24, 2018].

Denizman, C., 2018, Land-use changes and groundwater quality in Florida: Applied Water Science, v. 8, no. 5, Article 134, https://doi.org/10.1007/s13201-018-0776-9.

EPA (U.S. Environmental Protection Agency), 1981, Final Environmental Impact Statement for Mammoth Cave Area, Kentucky, Waste Water Facilities: U.S. EPA, 904/9-81-076, 156 p.

EPA (U.S. Environmental Protection Agency), 2018, Stormwater Phase II Final Rule Fact Sheet Series: https://www.epa.gov/npdes/stormwater-phase-ii-final-rule-fact-sheet-series, [accessed Oct. 16, 2020].

EPA (U.S. Environmental Protection Agency), 2019, EPA Interpretive Statement on the Application of the NPDES Program to Releases of Pollutants from Point Source to Groundwater: https://www.epa.gov/sites/production/files/2019-04/documents/interpretative_statement_fact-sheet_41519.pdf, [accessed Oct. 16, 2020].

Escolero, O.A., Marin, L.E., Steinich, B., Pacheco, A.J., Cabrera, S.A., and Alcocer, J., 2002, Development of a protection strategy of karst limestone aquifers: The Merida Yucatan, Mexico Case Study: Water Resources Management, v. 16, no. 5, p. 351−367, https://doi.org/10.1023/A:1021967909293.

Feist, S.K., Maclachlan, J.C., Reinhardt, E.G., and Skelding, H.S., 2020, Anthropogenic events captured within sediment in Hidden River Cave, Kentucky: Quaternary Science Advances, v. 1, no. 100001, https://doi.org/10.1016/j.qsa.2020.100001.

Fiorillo, F., 2016, Spring hydrograph recession: A brief review focused on karst aquifers: *in* Stevanović, Z., Krešić, N., and Kukurić, N., eds., Karst without Boundaries: Boca Raton, CRC Press, V. 23, p. 117−130, https://doi.org/10.1201/b21380-12.

Fleury, S., 2009, Land use policy and practice on karst terrains: Living on Limestone: New York, Springer, 187 p.

Ford, D.C., and Williams, P.W., 2007, Karst Geomorphology and Hydrology: Chichester, John Wiley & Sons, Ltd., 562 p.

Foster, D.G., 1999, Cave Management in the United States: An Overview of Significant Trends and Accomplishments: *in* Rea, G.T., ed., Proceedings of the 1999 National Cave and Karst Management Symposium, October 19−22: Chattanooga, Southeastern Cave Conservancy, p. 59−63.

Groves, C., Polk, J., Miller, B., Kambesis, P., Bolster, C., Vanderhoff, S., Tyrie, B., Ruth, M., Ouellette, G., Osterhoudt, L., Nedvidek, D., McClanahan, K., Lawhon, N., and Hall, H., 2013, The Western Kentucky University Crumps Cave Research and Education Preserve: *in* Land, L. and Joop, M.W., eds., 20th National Cave and Karst Management Symposium, October 4-9: Carlsbad, National Cave and Karst Research Institute, p. 105−110.

HCCC (Hart County Chamber of Commerce), 2013, Discover Hart County, Kentucky: https://www.hartcountyky.org/Directory_To_Print.pdf, [accessed Sept. 26, 2018].

HCPC (Hart County Planning Commission), 2007, Subdivision Regulations: Design and Development Standards: https://hartcountyky.org/wp-content/uploads/2019/12/subdivision.pdf, [accessed Oct. 18, 2020].

HCPC (Hart County Planning Commission), 2020, Hart County Comprehensive Plan Update 2020: https://www.klc.org/userfiles/files/Hart_County_Comp_Plan_Final_Web.pdf, [accessed Oct. 16, 2020].

Jarvis, T., Giordano, M., Puri, S., Matsumoto, K., and Wolf, A., 2005, International borders, ground water flow, and hydroschizophrenia: Groundwater, v. 43, no. 5, p. 764−770, https://doi.org/10.1111/j.1745-6584.2005.00069.x.

Jiang, Y., Cao, M., Yuan, D., Zhang, Y., and He, Q., 2018, Hydrogeological characterization and environmental effects of the deteriorating urban karst groundwater in a karst trough valley: Nanshan, SW China: Hydrogeology Journal, v. 26, no. 5, p. 1487−1497, https://doi.org/10.1007/s10040-018-1729-y.

KGA (Kentucky General Assembly), 2020, Kentucky Administrative Regulations: Title 401, Energy and Environment Cabinet – Department for Environmental Protection: https://apps.legislature.ky.gov/law/kar/TITLE401.HTM, [accessed Oct. 18, 2020].

KGS (Kentucky Geological Survey), 1997, Detailed Info About This Well (Casing & Lithologic), Kentucky Groundwater Data Repository: https://kgs.uky.edu/kgsweb/datasearching/water/wellinfo.asp?id=40004470&fromThickbox=true&height=450&width=600, [accessed Oct. 23, 2018].

Keranen, K., and Kolvoord, R., 2014, Making Spatial Decisions Using GIS and Remote Sensing: A Workbook: Redlands, Esri Press Academic, 300 p.

Knierim, K.J., Hays, P.D., and Bowman, D., 2015, Quantifying the variability in *Escherichia coli (E. coli)* throughout storm events at a karst spring in northwestern Arkansas, United States: Environmental Earth Sciences, v. 74, no. 6, p. 4607−4623, https://doi.org/10.1007/s12665-015-4416-5.

Lewis, J., 1995, The devastation and recovery of caves and karst affected by industrialization: *in* Rea, G.T., ed., Proceedings of the 1995 National Cave Management Symposium, Spring Mill State Park, October 25-28: Mitchell, National Cave Management Symposium Steering Committee, p. 214−227.

Li, G., Goldscheider, N., and Field, M.S., 2016, Modeling karst spring hydrograph recession based on head drop at sinkholes: Journal of Hydrology, v. 542, p. 820−827, https://doi.org/10.1016/j.jhydrol.2016.09.052.

Marín, L.E., Steinich, B., Pacheco, J., and Escolero, O.A., 2000, Hydrogeology of a contaminated sole-source karst aquifer, Mérida, Yucatán, Mexico: Geofísica International, v. 39, no. 4, p. 359−365, https://doi.org/10.22201/igeof.00167169p.2000.39.4.246.

McGrain, P., and Currens, J.C., 1978, Topography of Kentucky: Special Publication 25, Kentucky Geological Society, 76 p.

Meiman, J., Groves, C., and Herstein, S., 2001, Cave dye tracing and drainage basin divides in the Mammoth Cave Karst Aquifer, Kentucky: *in* Kuniansky, E.L., ed., U.S. Geological Survey Karst Interest Group Proceedings, St. Petersburg, FL, Feb. 2001: Reston, U.S. Geological Survey, p. 179−185.

Milanović, P., 2016, Optimal water management – Prerequisite for regional socio-economic development in the karst of the south-eastern Dinarides: I Stevanović, Z., Krešić, N., and Kukurić, N., eds., Karst without Boundaries: Leiden, CRC Press/Balkema, 364 p., https://doi.org/10.1201/b21380-11.

Murdoch, J., Bitting, C., and Van Brahana, J., 2016, Characterization of the karst hydrogeology of the Boone Formation in Big Creek Valley near Mt. Judea, Arkansas – documenting the close relation of groundwater and surface water: Environmental Earth Sciences, v. 75, no. 16, Article 1160, https://doi.org/10.1007/s12665-016-5981-y.

Nedvidek, D., 2014, Evaluating the Effectiveness of Regulatory Stormwater Monitoring Protocols on Groundwater Quality in Urbanized Karst Regions [M.S. thesis]: Bowling Green, Western Kentucky University, 136 p.

Osborne, C.N., 2018, Land-Use Impacts on the Hydrology of the Hidden River Groundwater Subbasin, Horse Cave, Hart County, Kentucky. [M.S. Geoscience thesis], Department of Geography and Geology, Western Kentucky University, Bowling Green, KY. Online at: https://digitalcommons.wku.edu/theses/3078/, https://doi.org/10.1130/abs/2018AM-324422.

Palmer, A.N., 1995, A Geological Guide to Mammoth Cave National Park: Teaneck, Zephyrus Press, 196 p.

Palmer, A.N., 2007, Cave Geology: Dayton, Cave Books, 454 p.

Quinlan, J.F., and Ewers, R.O., 1989, Subsurface drainage in the Mammoth Cave area: *in* White, W.B., and White, E.L., eds., Karst Hydrology: Concepts from the Mammoth Cave Area: New York, Van Nostrand Reinhold, 346 p, https://doi.org/10.1007/978-1-4615-7317-3_3.

Quinlan, J.F., and Rowe D.R., 1977, Hydrology and Water Quality in the Central Kentucky Karst: Phase I, University of Kentucky: Water Resources Research Institute, Report No. 101, 93 p.

Raedts, C., and Smart, C., 2015, Tracking of karst contamination using alternative monitoring strategies: Hidden River Cave, Kentucky: *in* Doctor, D.H., Land, L., and Stephenson, J.B., eds., Proceedings of the 14th Multidisciplinary Conference on Sinkholes and the Engineering and Environmental Impacts of Karst, Rochester, MN, Oct. 2015: Carlsbad, NM, National Cave and Karst Research Institute, p. 327−336, https://doi.org/10.5038/9780991000951.1055.

Ravbar, N., and Šebela, S., 2015, The effectiveness of protection policies and legislative framework with special regard to karst landscapes: insights from Slovenia: Environmental Science & Policy, v. 51, p. 106−116, https://doi.org/10.1016/j.envsci.2015.02.013.

Ray, J.A.,and Currens, J.C., 1998, Mapped Karst Ground-Water Basins in the Campbellsville 30 × 60 Minute Quadrangle: Lexington, Kentucky Geological Survey, Map and Chart Series 17, Series XI, 1:100,000, 2 p.

Richardson, J.J., 2018, Fitting regulatory square pegs into round holes: local land use regulation: *in* karst terrain: *in* White, W.B., Herman, J.S., Herman, E.K., and Rutigliano, M., eds., Karst Groundwater Contamination and Public Health: Beyond Case Studies: Berlin, Springer, 347 p.

Ryan, M., and Meiman, J., 1996, An examination of short-term variations in water quality at a karst spring in Kentucky: Groundwater, v. 34, no. 1, p. 23−30, https://doi.org/10.1111/j.1745-6584.1996.tb01861.x.

Schreiber, M.E., Schwartz, B.F., Orndorff, W., Doctor, D.H., Eagle, S.D., and Gerst, J.D., 2015, Instrumenting caves to collect hydrologic and geochemical data: case study from James Cave, Virginia: *in* Younos, T., and Parece, T.E., eds., Advances in Watershed Science and Assessment: Berlin, Springer, p. 205−231, https://doi.org/10.1007/978-3-319-14212-8_8.

Stevanović, Z., Kukurić, N., Pekaš, Ž., Jolović, B., Pambuku, A., and Radojević, D., 2016, Dinaric Karst Aquifer – One of the world's largest transboundary systems and an ideal location for applying innovative and integrated water management: *in* Stevanović, Z., Krešić, N., and Kukurić, N., eds., Karst Without Boundaries: Leiden, CRC Press/Balkema, 364 p., https://doi.org/10.1201/b21380-3.

Tagne, G.V., and Dowling, C., 2018, Inferring groundwater flow and recharge from time series analysis of storm responses in a karst aquifer of southeastern Kentucky (USA): Hydrogeology Journal, v. 26, no. 8, p. 2649−2668, https://doi.org/10.1007/s10040-018-1837-8.

Taylor, A., Curnow, R., Fletcher, T., and Lewis, J., 2007, Education campaigns to reduce stormwater pollution in commercial areas: do they work?: Journal of Environmental Management, v. 84, no. 3, p. 323−335, https://doi.org/10.1016/j.jenvman.2006.06.002.

Theesfeld, I., 2010, Institutional challenges for national groundwater governance: Policies and issues: Groundwater, v. 48, no. 1, p. 131−142, https://doi.org/10.1111/j.1745-6584.2009.00624.x.

Turpaud, P., Zini, L., Ravbar, N., Cucchi, F., Petrič, M., and Urbanc, J., 2018, Development of a protocol for the Karst Water Source Protection Zoning: Application to the classical karst region (NE Italy and SW Slovenia): Water Resources Management, v. 32, no. 6, p. 1953−1968, https://doi.org/10.1007/s11269-017-1882-4.

White, W.B., Watson, R.A., Pohl, E.R., and Brucker, R.W., 1970, The Central Kentucky Karst: Geographical Review, v. 60, p. 88-115, https://doi.org/10.2307/213346.

Wilson, J., and Rocha, C., 2016, A combined remote sensing and multi-tracer approach for localising and assessing groundwater-lake interactions: International Journal of Applied Earth Observation and Geoinformation, v. 44, p. 195−204, https://doi.org/10.1016/j.jag.2015.09.006.

Worthington, S.R.H., Ford, D.C., and Davies, G.J., 2000, Matrix, fracture and channel components of storage and flow in a Paleozoic limestone aquifer: *in* Sasowsky, I.D. and Wicks, C.M., eds., Groundwater Flow and Contaminant Transport in Carbonate Aquifers: Rotterdam, A.A. Balkema, 203 p.

Zhou, W., 2007, Drainage and flooding in karst terranes: Environmental Geology, v. 51, no. 6, p. 963−973, https://doi.org/10.1007/s00254-006-0365-3.